

The effect of changing the formation of multiple input multiple output antennas on the gain

Majed Omar Dwairi¹, Mohamed Salaheldeen Soliman^{2,3}, Amjad Yousef Hendi¹, Ziad AL-Qadi¹

¹Department of Electrical Engineering, Faculty of Engineering Technology Al-Balqa Applied University, Amman, Jordan

²Department of Electrical Engineering Faculty of Energy Engineering, Aswan University, Aswan, Egypt

³Department of Electrical Engineering, Faculty of Engineering, Taif University, Taif, Saudi Arabia

Article Info

Article history:

Received Nov 9, 2021

Revised Jul 30, 2022

Accepted Aug 20, 2022

Keywords:

Multiple input multiple output

Released gain

Resonant frequency

Return loss

Ultra-wideband

ABSTRACT

In this paper, different 2×1 and 2×2 multiple input multiple output (MIMO) antennas were investigated with changing substrate shapes and changing the placing of the patches on the substrate, all the investigated antennas based on FR-4 substrate are characterized by $\text{permittivity} = 4.4$, and loss $\text{tangent} = 0.02$, with a partial ground. The original antenna covered 3.4 to 13.5 GHz. The best simulation results of the proposed 2×1 MIMO antenna received for 2×1 inverted with high ultra-wideband (UWB) with bandwidth up to 40 GHz, the received maximum gain was up to 6.51 dB, with an average gain of more than the original single antenna at about +1.27 dB. The best of eight 2×2 MIMO antennas configurations that give good results were shown. The best-received gain compared with a single antenna gain were at 4.2 GHz about +2.73, +1.17, and +0.92 dB for plus-shaped, loop, and chair-shaped respectively. A comparison between the proposed MIMO antennas and other reported works were done. The proposed MIMO antennas give a good maximum gain and are suitable for different narrow bands within the UWB such as wireless local area network (WLAN), worldwide interoperability for microwave access (WiMAX), aeronautical radio navigation (ARN), International Telecommunication Union 8-GHz (ITU-8), and X-Band applications with the ability to give high gain without the need to increase the radiated power of the transmitter antenna.

This is an open access article under the [CC BY-SA](https://creativecommons.org/licenses/by-sa/4.0/) license.



Corresponding Author:

Majed Omar Dwairi

Department of Electrical Engineering, Faculty of Engineering Technology Al-Balqa Applied University

P.O. Box: 15008 Amman 11134, Jordan

Email: majeddw@bau.edu.jo

1. INTRODUCTION

Nowadays, ultra-wideband (UWB) micro strip antenna design plays an important role in modern microwave antenna design; researchers give it more attention after UWB (3.1 to 10.6) GHz was licensed by the Federal Communication Commission (FCC) [1]. The importance of using micro strip antenna is due to its several advantages compared with other microwave antennas such as low profile, light weight, low cost, capability of many frequency operations, and ease of integration with microwave integrated circuit. Many simulation tools were introduced to microstrip antenna design such as: CST, HFSS, FEKO, IE3D, and others that gave the researchers the possibility to work in this direction and obtain results close to the reality of the antenna to be manufactured and adjust and improve it before manufacturing, to reach the required antenna with accuracy and effectiveness. Some different parameters were investigated to determine the operated, mismatched, and rejected bands such as those which were investigated Soliman *et al.* [2]. Moreover, to study the effect of inserting different slots within the patch or ground or both of them, Dwairi *et al.* [3] proposed

twenty different fractal slots shaped on the patch studying the effect of these slots on the operating bandwidth and decreasing the patch area, in addition, to studying the effect of their different fractal slots on the different parameters. Soliman *et al.* [4] were investigated a compact UWB antenna using different ground slots to enhance the operating bandwidth, the authors received bandwidth up to 31.1 GHz with a relative bandwidth of about 164%. Alotaibi and Alotaibi [5] a triple-band notched filter was proposed using different slots shaped were used U, T, and L-shaped slots used for worldwide interoperability for microwave access (WiMAX), wireless local area network (WLAN), and X-Band used respectively to achieve the desired notch filter. Al-Dwairi [6] proposed for filters with different slot configuration on the patch, feed, and the ground receiving reject filters for WiMAX operating bandwidth 93.3-3.7GHz, aeronautical radio navigation (ARN) operating bandwidth 4.2 to 4.5 GHz, WLAN operating bandwidth 5.15 to 5.825GHz, and X-Band (a segment of the superhigh-frequency radio spectrum that lies between 5.2 GHz and 10.9 GHz and is used especially for radars and for spacecraft communication, our investigating bandwidth 7.25 to 7.75). Al-Dwairi *et al.* [7] proposed five band notched filters using U, S, and Σ -shaped on the patch, feed, and ground receiving WiMAX, ARN, WLAN, X-Band, and the International Telecommunication Union 8-GHz (ITU-8). In [8]–[11] the authors use different slots in the patch of the antenna or in its ground or on both, which were inserted to eliminate unwanted narrow frequency bands within the operating UWB, known as filters, receiving 3, 4, and 5 notched filters, such as in [10] received four rejection band filters using a very small factor UWB microstrip antenna are proposed to be used in internet of things (IoT), and in mobile communication, receiving five rejection bands for bandwidth from 3.5 to 8.2 GHz.

Multiple input multiple output (MIMO) antennas were introduced to micro strip antenna to improve the data throughput, range, and gain for the received antenna without the need to increase the transmitted power or its bandwidth, many works concentrated on this type of design such as Weng and Chu [12] were choosing an optimized size and location of the slot on the feeding line receiving a high gain MIMO antenna that is designed for mm-wave applications. The most challenging thing for MIMO antennas designer is the mutual coupling effect that changes the input impedance of the individual antenna elements in an array and therefore, changes the pattern of the antenna operation and degrades the performance of the array. Many techniques and methods to reduce the mutual coupling depending on the application of the investigated antennas and the way of excitation have been produced.

Alibakhshikenari *et al.* [13] produced a 2×2 MIMO antenna operating in three narrow bands from 2.11-4.42 GHz with reduced mutual coupling by implementing a proper slot on the partial ground and increasing the efficiency up to 73% on the resonant frequencies. Alibakhshikenari *et al.* [14], [15] produced different aperture-coupling and defected ground structures (DGS) to increase the insulation from the patch and the feeding element; in [14] the aperture-coupling was used to isolate the micro strip by inserting T-shaped and orthogonally around the squared patch, the produced antenna is applicable for WLAN communication, while in [15] two circular patch antennas are closely placed to each other and inserted H-shaped DGS on the ground that highly decreases the mutual coupling, producing MIMO antenna that operates at 5.3 GHz frequency, which can be used for Wi-Fi and WiMAX. Microstrip antennas have various applications for wireless communication systems using different microstrip antenna designs and configurations for different applications.

Alibakhshikenari *et al.* [16] designed a 4-pair conformal micro strip MIMO antenna consisting of eight cells each operating in ka-band (35 GHz), resulting in a reduction of the side lobe at the same time of increasing the bandwidth; the simulated and measured results conformed. Alibakhshikenari *et al.* [17] introduced a 5G handset mobile communication antenna using a compact 2×2 MIMO patch antenna that characterizes by a super wideband starting from 2.97 to 19.82 GHz, this proposed antenna achieved a gain of more than 8 dB. Swamy and Siddaiah [18], a 4-element MIMO patch antenna with inset line feeding was investigated for narrowband from 27 to 28.95 GHz. The received results proved a reduction of BER at the same time increasing the signal to noise ratio, and the resulting gain received was about 6.14 dB, with the perspective to use this produced antenna for 5G mobile handset antenna application. Li *et al.* [19], a modified pentagonal micro strip antenna was investigated and introduced a high gain of about 6.17 dB with a perspective to be used for 5G applications. Khan *et al.* [20], the author shows that the gain improvement of the proposed 2×2 MIMO antenna were from 1 to 2.5 dB, that has been achieved compared to the single patch antenna. Alibakhshikenari *et al.* [21] proposed UWB antenna to exhibit excellent radiation characteristics, using F and T-shaped slots on the ground and the arms respectively, receiving relative bandwidth of about 173% and a maximum gain 3.5 dBi.

Alibakhshikenari *et al.* [22] a very useful survey was presented with a comprehensive study of deferent methods with different isolation based on meta surface inspired and metamaterial for antennas and analyze each of the presented methods. In [23] reduced unwanted mutual coupling for 34 by 34 antenna array by using substrate-integrated-waveguide (SIW) for operating at THz band, which is realized by interjecting metallic via-holes between the radiating elements to block propagating surface waves. Alibakhshikenari *et al.*

[24] used metamaterial photonic bandgap techniques to reduce mutual coupling which is simple and effective. Alibakhshikenari *et al.* and Wang *et al.* [25], [26] an effective technique is used for suppressing the mutual coupling based on a metamaterial (MTM) electromagnetic bandgap. Alsoif [27] a UWB microstrip antenna has been proposed for portable wireless devices based on a simplified composite right/left-hand transmission line, this antenna was implemented using F and T-shaped slots in the patch radiator, the operating bandwidth operates from 0.6 to 9.2 GHz giving relative bandwidth of about 173.6% and gains about 4 dBi. Proposed and investigated important antennas works based on metamaterials, for UWB portable microwave devices and wireless communications [28]–[30].

In this paper, an UWB antenna based on [8], was optimized to operate at UWB, then the authors inserted some slots within the patch and the feed line to reject WLAN and X-bands. The proposed antenna in [8] is a good candidate for our investigation to be modified to MIMO scenarios with 2×1 and 2×2 , with different modifications to compare these MIMO antennas and discover which gives the best gain. The remainder of this work has been organized as follows: section 2 single antenna design, next section 3 simulation results of 2×1 and 2×2 MIMO antennas; section 4 discussion of the received results. Finally, conclusions and future work were discussed in section 5.

2. ANTENNA DESIGN

The investigated UWB micro strip patch antenna based on [8], is presented in Figures 1(a) to (c), the substrate is built on FR4 with relative permittivity equal to 4.4 and loss tangent equal to 0.02. The antenna dimensions are listed in Table 1. In order to improve the patch antenna bandwidth and its matching inserted an arc cut of radius R mm at the corners of the rectangular patch antenna and the cutting polygonal slot in the ground, which in turn neutralized the capacitive and inductive reactance receiving a pure resistive input impedance [8]. The best slot cut circles at the rectangular angles are $R_1=R_2=R_3=R_4=2$ mm. The polygonal dimensions are listed in Table 1. This produced antenna will be modified to different 2×1 and 2×2 MIMO antennas and all the comparisons of the investigated MIMO antennas will be referred to this original antenna in point of view return loss and the released gain.

Table 1. Antenna parameters

	Length [mm]	Width [mm]	Height [mm]
Substrate	$L_s = 35$	$W_s = 30$	$H_s = 1.6$
Patch antenna	$L_p = 14.5$	$W_p = 15$	$t_p = 0.009$
Feed line	$L_f = 13.5$	$W_f = 2.85$	
Ground	$L_g = 12.5$	$W_g = 30$	
Ground slot	polygonal shape with $w = 3\text{mm}$, $L = 0.75\text{mm}$ and $L_1 = 1\text{mm}$		

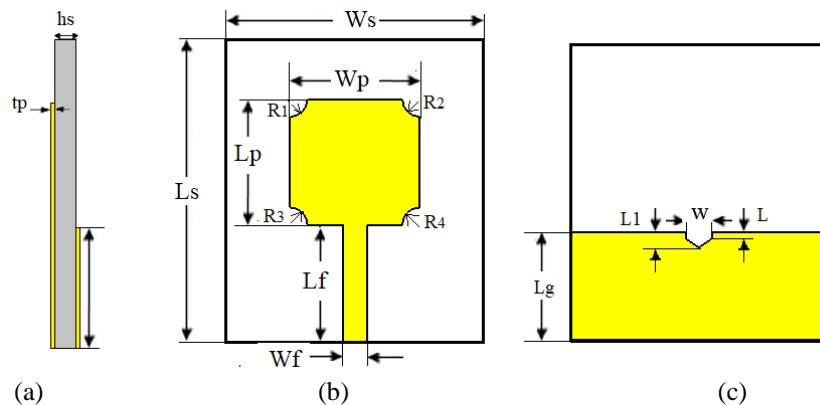


Figure 1. The investigated antenna: (a) side view, (b) front view, and (c) back view

3. SIMULATION RESULTS

The simulation of the investigated single antenna and the all-proposed MIMOs antennas has been carried out using CST-EM simulator 2018, where all the investigated antennas are based on the reference antenna introduced in [8]. The investigation started with the simulation of the original antenna followed by the three proposed 2×1 MIMO antennas designed and the results. Finally, an investigation of the eight proposed 2×2 MIMO antennas designed and results.

3.1. Single antenna results

Equations should be placed at the center of the line and provided consecutively with equation numbers. The investigated single antenna based on [8], shown in Figure 1. The simulation results of the return loss (S11), voltage standing wave ratio (VSWR), and the released gain are shown in Figures 2 to 4. The operating bandwidth for all proposed antennas has been from 2 to 15 GHz.

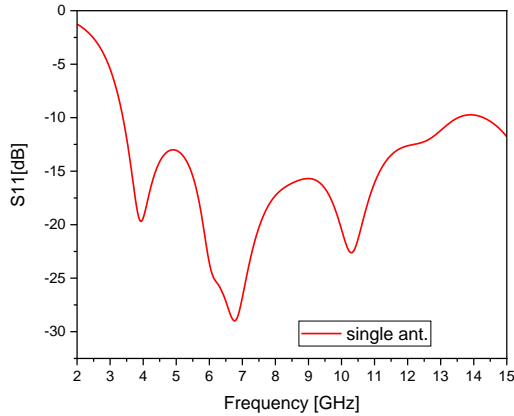


Figure 2. The simulated return loss for the single antenna

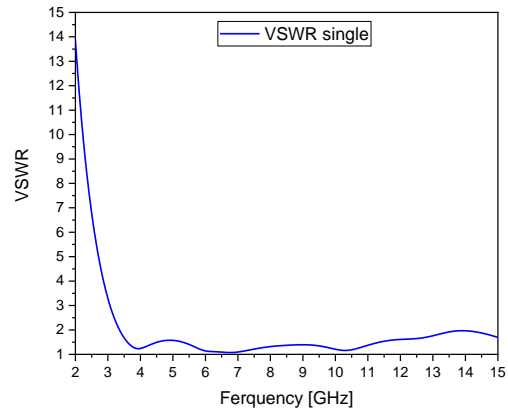


Figure 3. The simulated VSWR for the single antenna

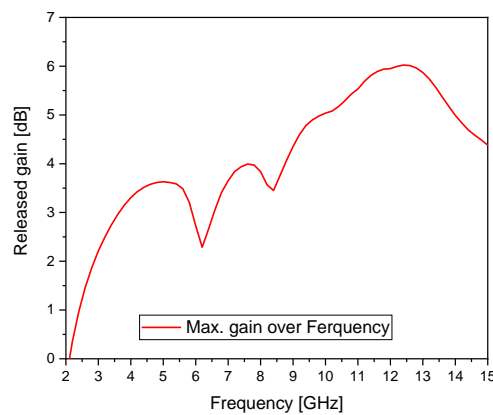


Figure 4. The simulated released gain for the single antenna

3.2. 2×1 MIMO antenna results

Three different 2×1 antenna configuration was investigated based on changing the dimensions of the substrate and the location of the patch antenna on the substrate. The investigated are shown in Figures 5(a) to 5(c), where the first 2×1 antenna was introduced as inverted MIMO, the second 2×1 was introduced as mirrored MIMO, and finally, the third 2×1 antenna was introduced as nearby MIMO. For all the investigated 2×1 MIMO antennas we found the return loss and the gain; which will be later compared in the discussion section.

3.2.1. 2×1 Inverted MIMO antenna

The proposed 2×1 inverted MIMO antenna is the modified single antenna substrate dimension $(2W_s + 2\text{mm} \times L_s \times h_s)$ mm³, as shown in Figure 5(a). The two antennas are the same dimensions inverted 180 degrees with 2 mm inserted in the substrate width to separate the ground of the two antennas. The simulation results of the return loss S11, S22, S12, and S21 (where S12, and S21 are the coupling return loss), and the released gain are shown in Figures 6 and 7 respectively. In Figure 7, it is seen that S11 and S22 are identical and S12 and S21 are identical as well. From S-parameters, it is notable that the bandwidth is received up to 40 GHz without any mismatched or rejected band; this is the only case that received these results. From Figure 7, the overall released gain of the bandwidth is good.

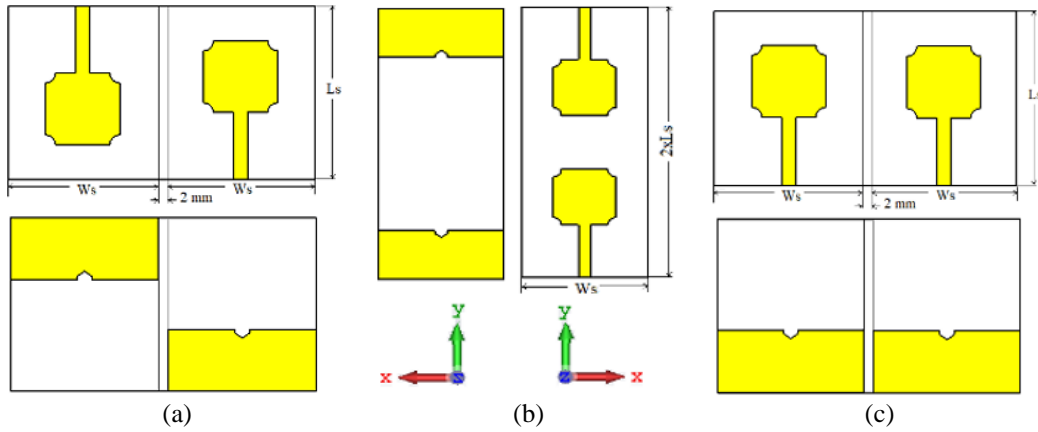


Figure 5. 2×1 MIMO antennas, (a) inverted, (b) mirrored, and (c) nearby

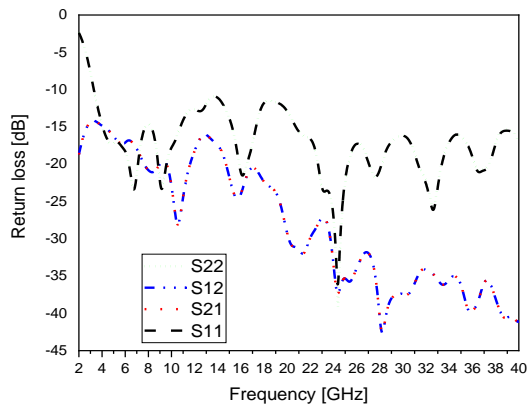


Figure 6. The simulated return loss S11, S22, and coupling S12, and S21 for 2×1 inverted MIMO antenna

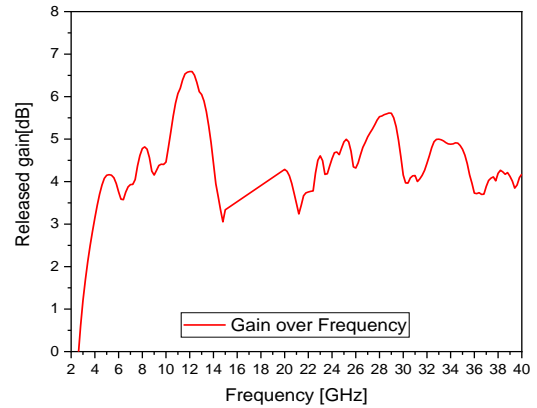


Figure 7. The simulated released gain for 2×1 inverted MIMO antenna

3.2.2. 2×1 mirrored MIMO antenna

The 2×1 mirrored MIMO antenna is shown in Figure 5(b), the modification is done by doubling the substrate length, with the same width. The second patch antenna is the same dimensions but mirrors the first. The simulation results of the return loss S₁₁, S₂₂, S₁₂, and S₂₁, and the released gain are shown in Figures 8 and 9, respectively.

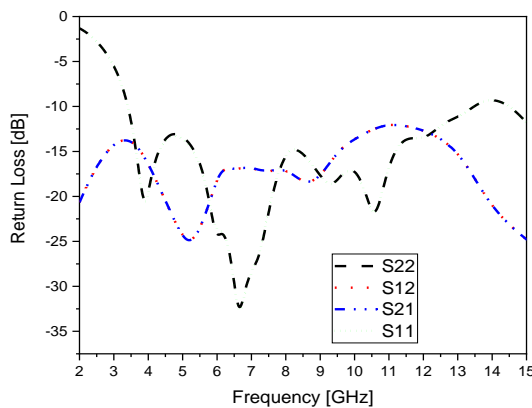


Figure 8. the simulated return loss S₁₁, S₂₂, and coupling S₁₂, and S₂₁ for 2×1 mirrored MIMO antenna

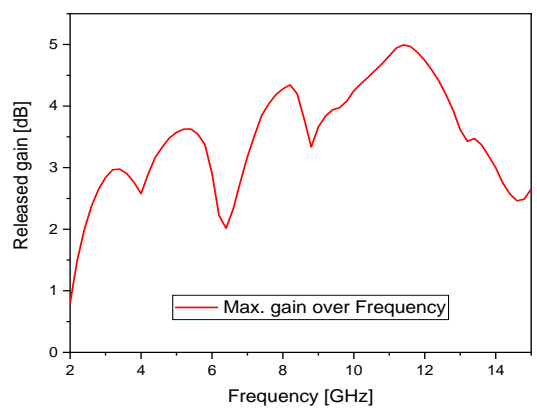


Figure 9. The simulated released gain for 2×1 mirrored MIMO antenna

3.2.3. 2×1 nearby MIMO antenna

The 2×1 nearby MIMO antenna is shown in Figure 5(c), the modification is done by doubling the substrate width and adding 2mm to separate the ground of antennas, with the same antenna length. The second patch antenna is the same dimensions nearby the first. The simulation results of the return loss S11, S22, S12, and S21, and the released gain are shown in Figures 10 and 11 respectively.

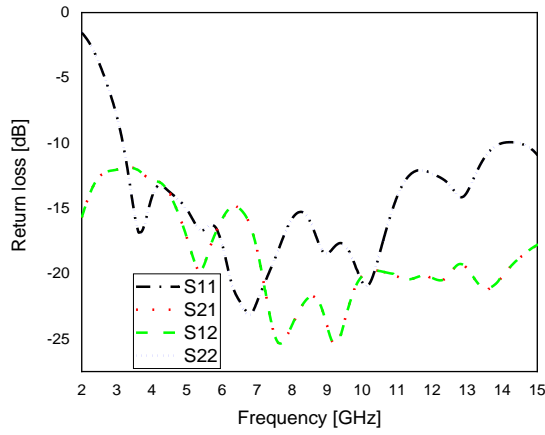


Figure 10. The simulated return loss S11, S22, and coupling S12, and S21 for 2×1 nearby MIMO antenna.

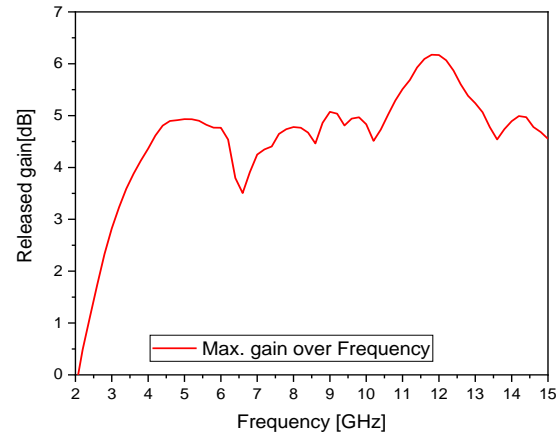


Figure 11. The simulated released gain for 2×1 nearby MIMO antenna

3.3. 2×2 MIMO antennas results

Eight 2×2 antenna configuration designs were a comparison will investigated with different antenna location on the substrate as shown in Figures 12(a) to (d), Figures 13(a) to (d), Figures 14(a) to (d), and Figures 15(a) to (d). The investigation was carried out for all MIMO antennas for return loss and released gain that will be compared in the discussion section. A comparison will be carried out in the discussion section.

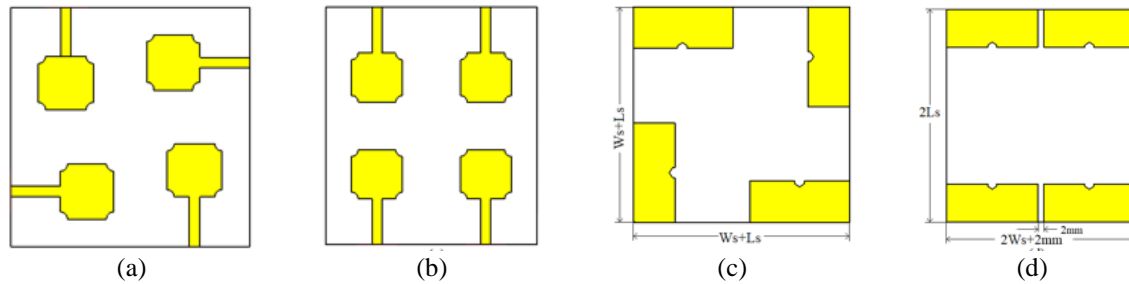


Figure 12. 2×2 MIMO antennas, (a) and (b) front and back views 2×2 loop MIMO, (c) and (d) front and back views 2×2 mirrored MIMO

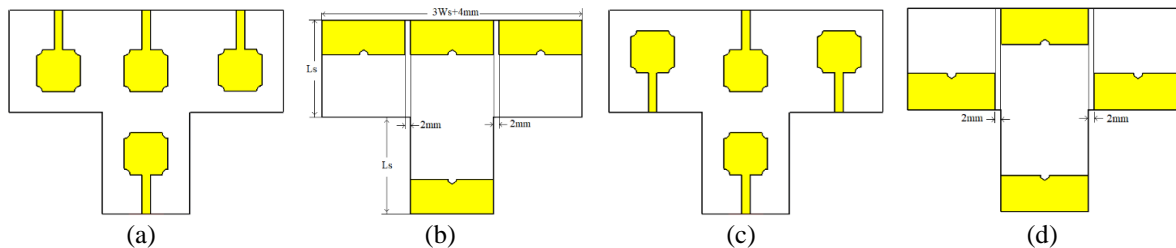


Figure 13. 2×2 MIMO antennas, (a) and (b) front and back views 2×2 T-Mirrored MIMO, (c) and (d) front and back views 2×2 T-mirrored center inverted MIMO

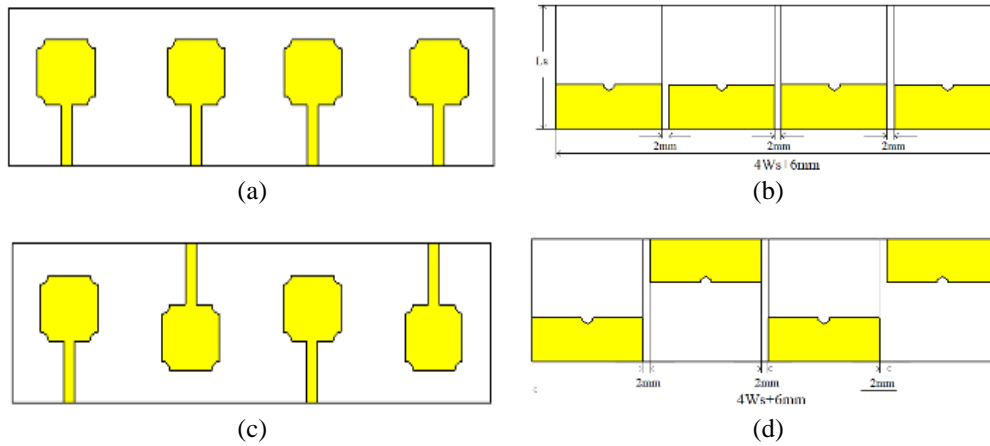


Figure 14. 2×2 MIMO antennas, (a) and (b) front and back views 2×2 nearby MIMO, (c) and (d) front and back views 2×2 nearby inverted MIMO

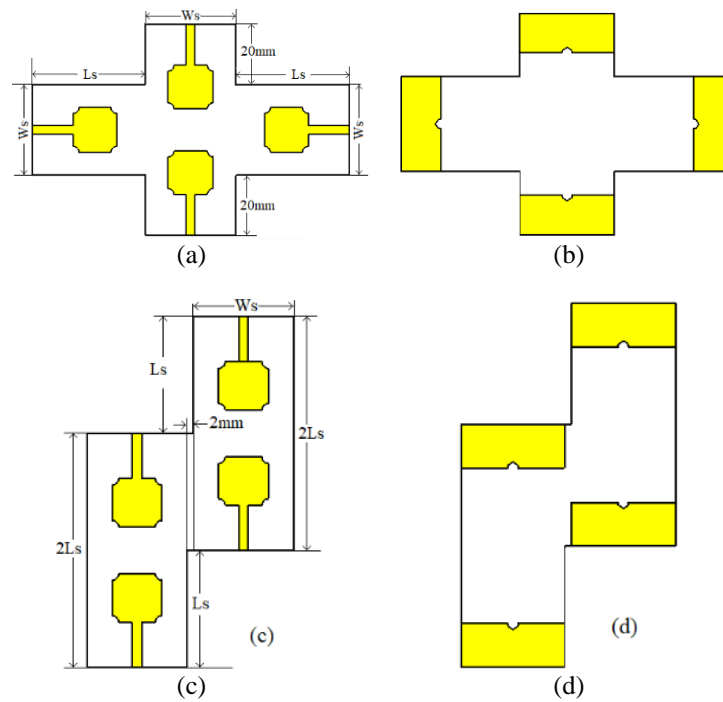


Figure 15. 2×2 MIMO antennas, (a) and (b) front and back views 2×2 plus shaped MIMO, (c) and (d) front and back views 2×2 chair-shaped MIMO

3.3.1. 2×2 loop MIMO antenna results

The 2×2 loop MIMO antenna configured as shown in Figures 12(a) front view and 12(b) back view. Where the dimension of the substrate is increased to (W_s+L_s) squared. The next antenna is placed 90 degrees left to the previous one and shifted up to a substrate length, as shown in Figure 13(a). Figures 16 to 18 show return loss, return loss of coupling antenna, and released gain respectively. Figure 18 showed both gains for single antenna and 2×2 loop MIMO, to demonstrate the difference in one figure.

3.3.2. 2 × 2 Mirrored MIMO antenna results

The 2×2 Mirrored MIMO antenna configured as shown in Figures 12(c) front view and 12(d) back view. Where the dimension of the substrate is changed to double length $(2L_s)$ and the width is changed to the double of the substrate width with adding 2 mm, in order separate the ground of the patches from each other $(2 W_s+2 \text{ mm})$. The configuration of this antenna is done by inserting two patches nearby with 2 mm separation and mirroring the other two antennas. Figures 19 to 21 show return loss, return loss of coupling antenna, and

released gain respectively. From Figure 19, it is evident that all the return losses are identical. Figure 21 showed both gains for single antenna and 2x2 loop MIMO, to demonstrate the difference in one figure.

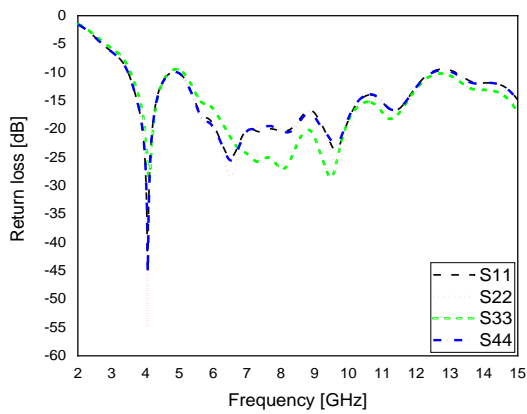


Figure 16. Return loss S11, S22, S33, and S44 for 2x2 loop MIMO

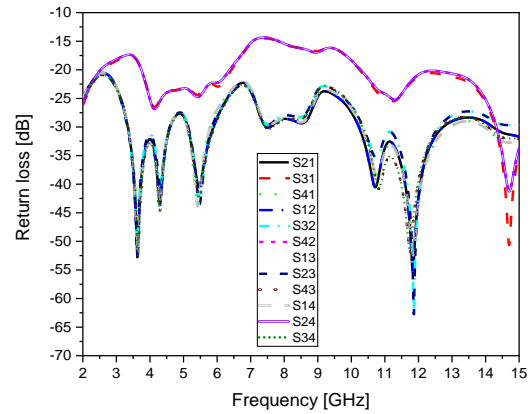


Figure 17. Return loss coupling S12, S13, S14, S21, S23, S24, S31, S32, S34, S41, S42, and S43 for 2x2 loop MIMO

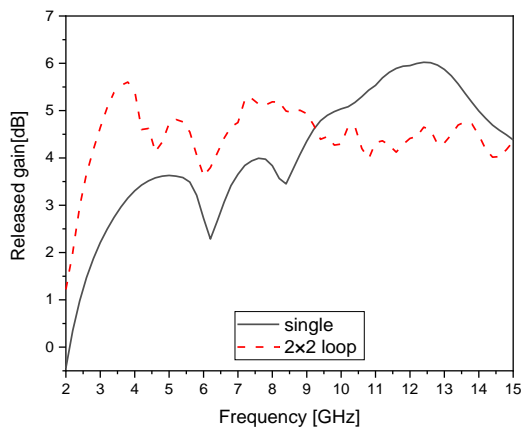


Figure 18. Released gain single and 2x2 loop MIMO antenna

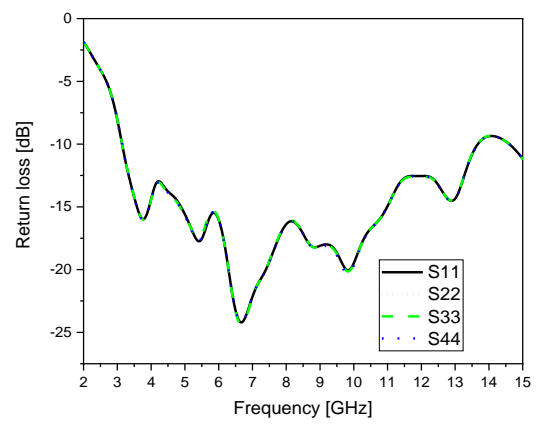


Figure 19. Return loss S11, S22, S33, and S44 for 2x2 mirrored MIMO

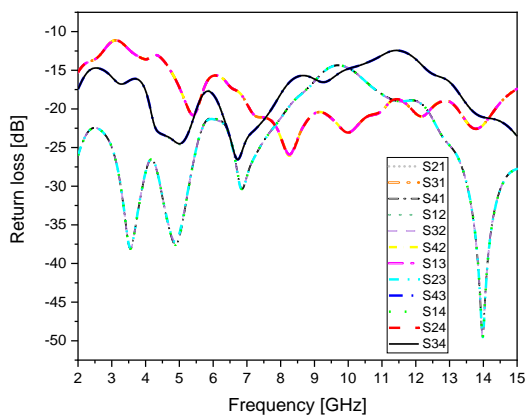


Figure 20. Return loss coupling S12, S13, S14, S21, S23, S24, S31, S32, S34, S41, S42, and S43 for 2x2 mirrored MIMO

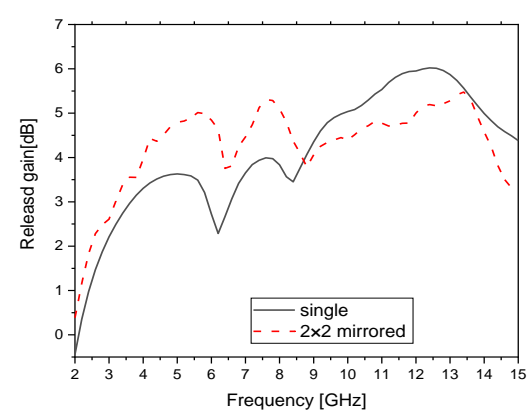


Figure 21. Released gain single, and 2x2 mirrored MIMO antenna

3.3.3. 2x2 T-Mirrored MIMO antenna results

The 2x2 T-Mirrored MIMO antenna is configured as shown in Figures 13(a) front view and 13(b) back view. The shape of this MIMO antenna is T-shaped, where the dimension of the substrate is changed to double length (2Ls) and the width is changed to the triple of the substrate width with adding 4 mm (3 Ws+4 mm). The upper antennas are in the same direction but are mirroring the base antenna. Figures 22 to 24 show return loss, return loss of coupling antenna and released gain respectively. From Figure 22 it is evident that S22 and S33 are identical, whereas S11 and S44 are different. Figure 23 showed both gains for a single antenna and 2x2 T-shaped MIMO.

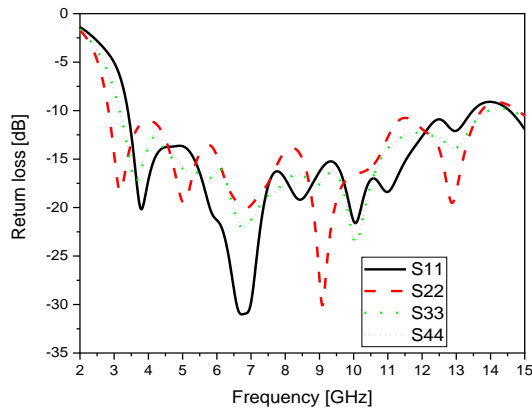


Figure 22. Return loss S11, S22, S33, and S44 for 2x2 T-mirrored MIMO

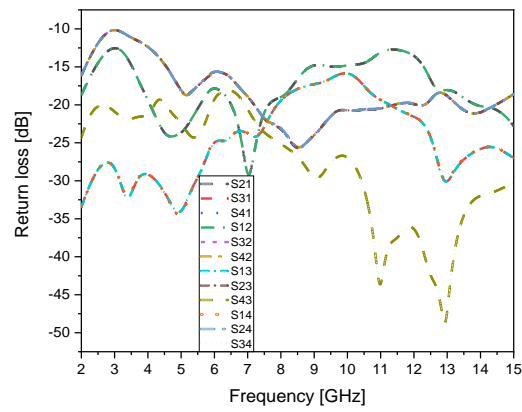


Figure 23. Return loss coupling S12, S13, S14, S21, S23, S24, S31, S32, S34, S41, S42, and S43 for 2x2 T-mirrored MIMO

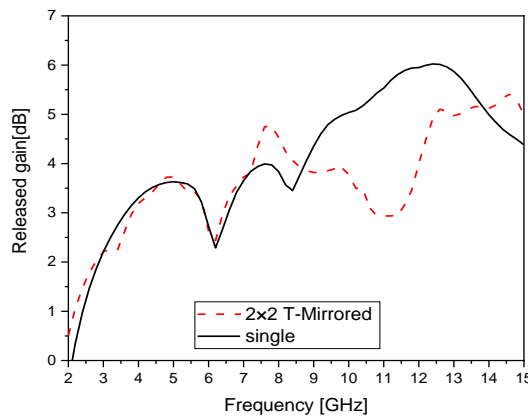


Figure 24. Released gain single, and 2x2 T-mirrored MIMO antenna

3.3.4. 2x2 T-Mirrored center inverted MIMO antenna results

The proposed simulation 2x2 T-Mirrored center inverted MIMO antenna is configured as shown in Figures 13(c) front view and 13(d) back view. The shape and dimensions of this MIMO antenna is the same as T-mirrored Figures 13(a) and 13(b), with one difference where outer upper antennas are in the same direction as the lower base antenna. Figures 25 to 27 show return loss, return loss of coupling antenna and released gain respectively. From Figure 25 it is evident that S33 and S44 are identical, whereas S11 and S22 are different. Figure 27 shows both gains for a single antenna and 2x2 T-shaped MIMO. In Figure 28 a comparison of released gain was made between T-shaped and this antenna; as evident, this T-mirrored center inverted MIMO antenna configuration gives better gain over the operating UWB.

3.3.5. 2x2 nearby MIMO antenna results

The 2x2 nearby MIMO antenna is configured as shown in Figures 14(a) front view and 14(b) back view. The shape and dimensions of this MIMO antenna is done by increasing the width of the substrate four

times with adding 2 mm spacing between neighboring antennas (4 W_s+6 mm), with the same substrate length (L_s). Figures 29 to 31 show return loss, return loss of coupling antenna and released gain respectively. From Figure 29 it is evident that S_{11} and S_{22} are identical, and that S_{33} and S_{44} are identical as well. Figure 30 shows both gains for a single antenna and 2×2 nearby MIMO.

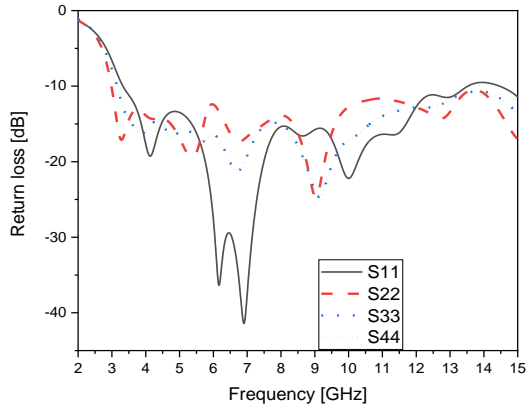


Figure 25. Return loss S_{11} , S_{22} , S_{33} , and S_{44} for 2×2 T-mirrored center inverted MIMO

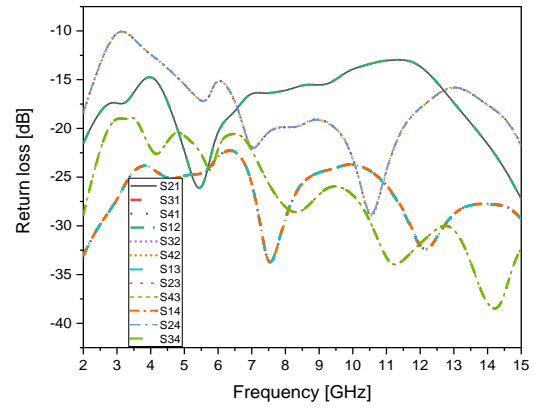


Figure 26. Return loss coupling S_{12} , S_{13} , S_{14} , S_{21} , S_{23} , S_{24} , S_{31} , S_{32} , S_{34} , S_{41} , S_{42} , and S_{43} for 2×2 T-mirrored center inverted MIMO

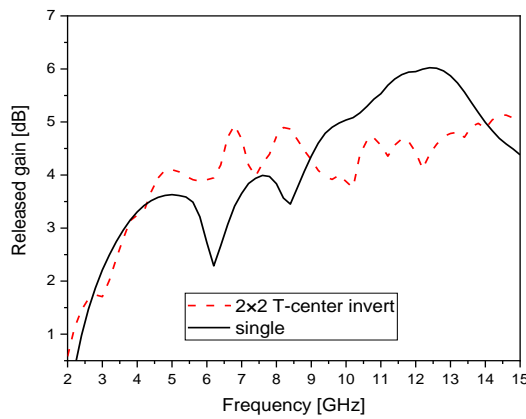


Figure 27. Released gain single and 2×2 mirrored center inverted MIMO antenna

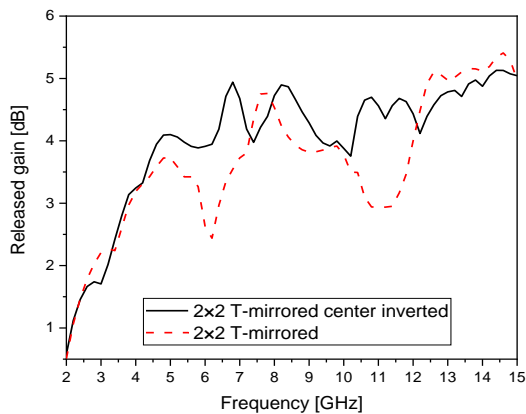


Figure 28. Comparison released gain 2×2 T-mirrored and 2×2 T-mirrored center inverted MIMO antenna

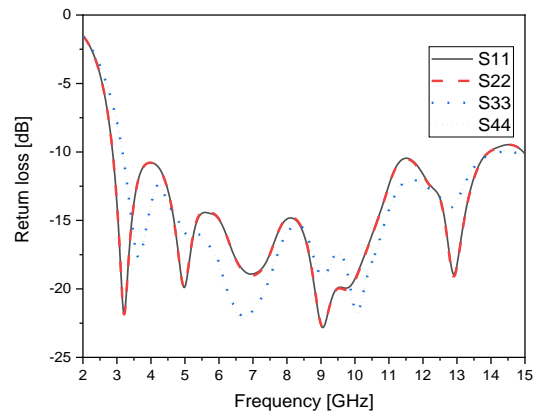


Figure 29. Return loss S_{11} , S_{22} , S_{33} , and S_{44} for 2×2 nearby MIMO

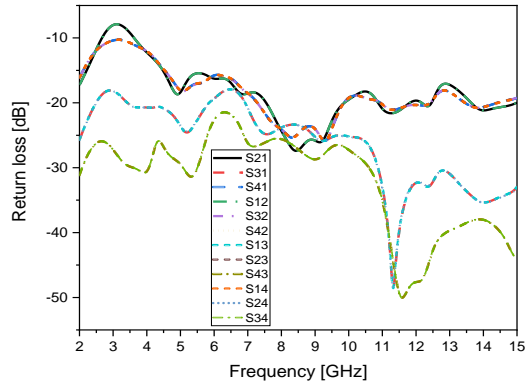


Figure 30. Return loss coupling S12, S13, S14, S21, S23, S24, S31, S32, S34, S41, S42, and S43 for 2×2 nearby MIMO

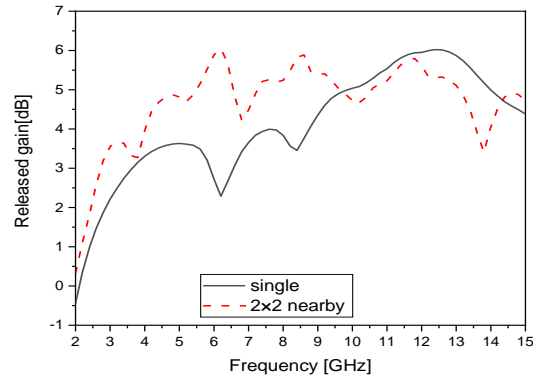


Figure 31. Released gain single, and 2×2 nearby MIMO antenna

3.3.6. 2×2 nearby-inverted MIMO antenna results

The proposed 2×2 nearby inverted MIMO antenna is configured as shown in Figures 14(c) front view and 14(d) back view. The shape and dimensions of this MIMO antenna are the same as 2×2 nearby MIMO antenna except that every antenna is an inverted version of the nearby one. Figures 32 to 34 show return loss, return loss of coupling antenna and released gain respectively. From Figure 32 it is evident that S11 and S22 are identical, and that S33 and S44 are identical as well. Figure 35 shows a comparison between the released gain of 2×2 nearby and 2×2 nearby-inverted MIMO antenna.

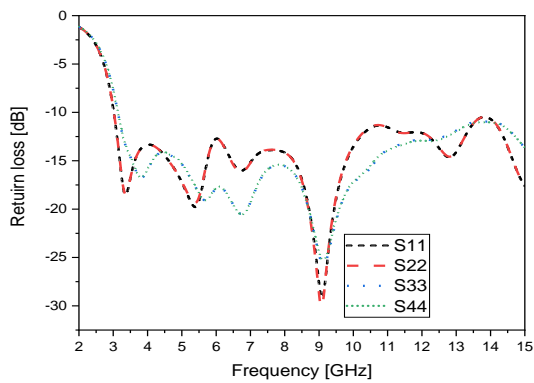


Figure 32. Return loss S11, S22, S33, and S44 for 2×2 nearby inverted MIMO

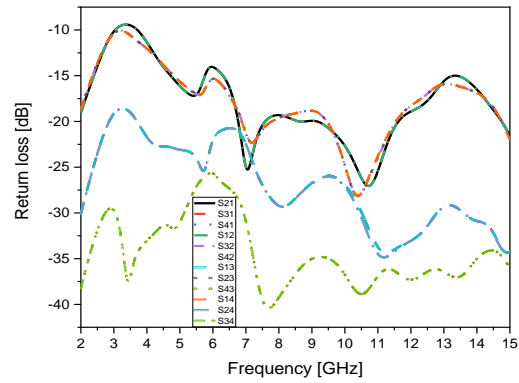


Figure 33. Return loss coupling S12, S13, S14, S21, S23, S24, S31, S32, S34, S41, S42, and S43 for 2×2 nearby inverted MIMO

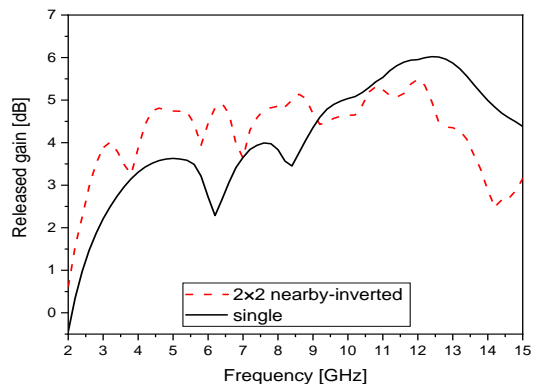


Figure 34. Released gain single and 2×2 nearby inverted MIMO antenna

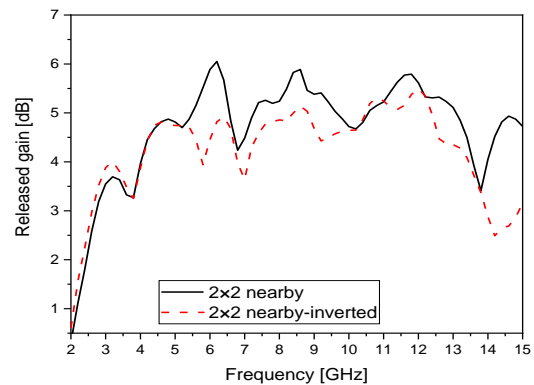


Figure 35. Comparison released gain 2×2 nearby and 2×2 nearby-inverted MIMO antenna

3.3.7. 2x2 plus-shaped MIMO antenna results

The proposed 2x2 plus-shaped MIMO antenna is configured as shown in Figures 15(a) front view and 15(b) back view. The shape of this MIMO antenna is done like a plus-shape where the dimensions are formed in a way that the width is twice the original substrate length plus the substrate width (2Ls+Ws), and the length is the original substrate antenna width plus 40 mm (Ws+40 mm). Figures 36 to 38 shown return loss, return loss of coupling antenna, and released gain respectively. From Figure 36 it is evident that S11 and S22 are identical and that S33 and S44 are identical as well. Figure 38 shows both gains for a single antenna and 2x2 nearby MIMO.

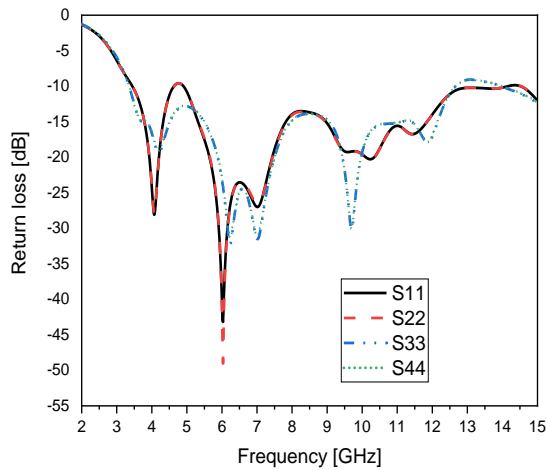


Figure 36. Return loss S11, S22, S33, and S44 for 2x2 plus-shaped MIMO

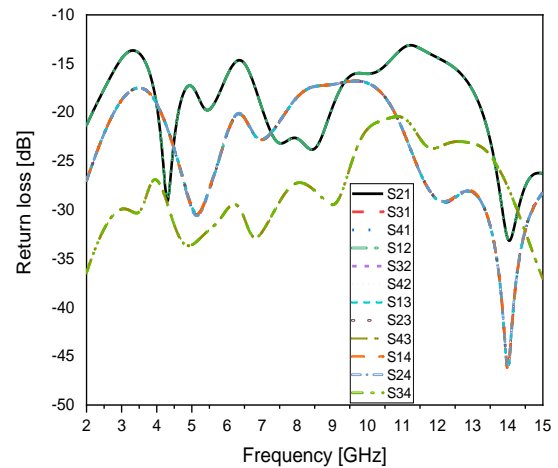


Figure 37. Return loss coupling S12, S13, S14, S21, S23, S24, S31, S32, S34, S41, S42, and S43 for 2x2 plus-shaped MIMO

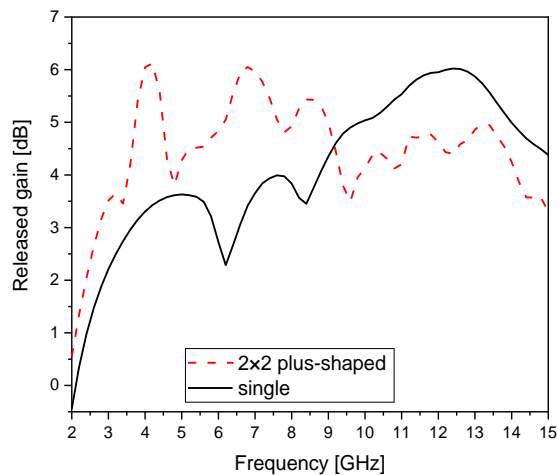


Figure 38. Released gain single and 2x2 plus-shaped MIMO antenna

3.3.8. 2x2 chair-shaped MIMO antenna results

The 2x2 chair-shaped MIMO antenna is configured as shown in Figures 15(c) front view and 15(d) back view. The shape of this MIMO antenna is done like a chair-shape where the dimensions are formed that the width is twice the original substrate length plus 2 mm (2 Ws+2 mm), and the length is twice of the original substrate (2Ls). Figures 39 to 41 show return loss, return loss of coupling antenna and released gain respectively. From Figure 39 it is evident that S11 and S22 are identical and that S33 and S44 are identical as well. Figure 41 shows both gains for a single antenna and 2x2 chair-shaped MIMO. Figure 42 shows a Comparison between the released gain of 2x2 nearby and 2x2 nearby-inverted MIMO antenna.

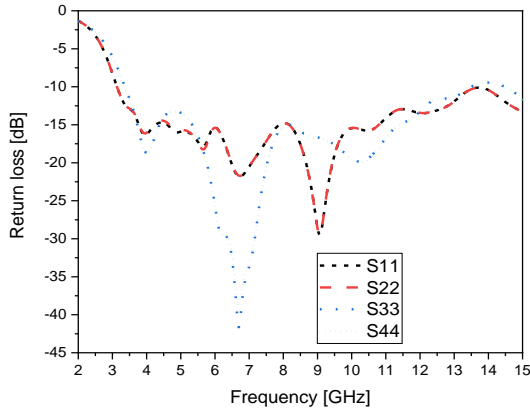


Figure 39. Return loss S11, S22, S33, and S44 for 2x2 chair-shaped MIMO

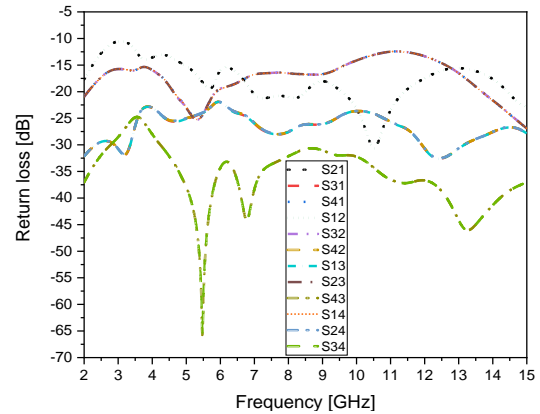


Figure 40. Return loss coupling S12, S13, S14, S21, S23, S24, S31, S32, S34, S41, S42, and S43 for 2x2 chair-shaped MIMO

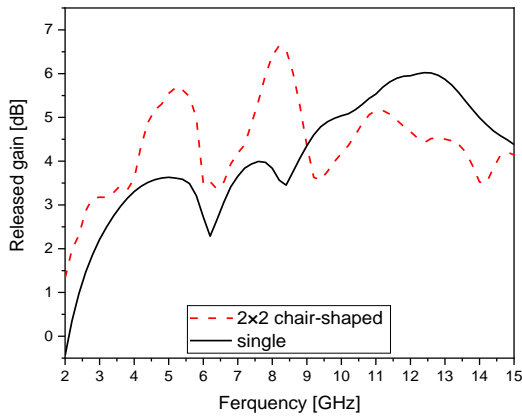


Figure 41. Released gain single and 2x2 chair-shaped MIMO antenna

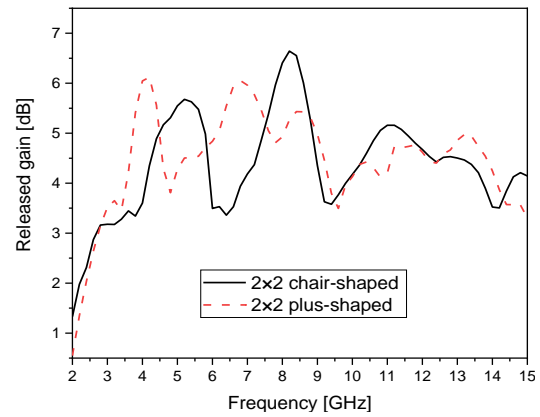


Figure 42. Comparison released gain 2x2 plus-shaped and 2x2 chair-shaped MIMO antenna

4. DISCUSSIONS OF THE RECEIVED RESULTS

The main purpose of this paper is to use the MIMO patch antenna to increase the released gain without the need to increase the power radiated from the antenna. The investigation was done on three 2x1 MIMO antennas, and eight 2x2 MIMO antennas. The discussion will be as follows: first, comparison of the original single antenna with all the MIMO antennas from the point of view of the operating UWB bandwidth; then, comparison of the single antenna released gain with 2x1 MIMO antennas; comparison of original antenna with 2x2 MIMO antennas; compare our results with other reported works, and finally, evaluation of the best-released gain

4.1. UWB operating bandwidth

A composition between the original antenna and all other investigated MIMO antennas from the point of view of the operating UWB bandwidth, resonant frequencies, and relative bandwidth, is listed in. The operating bandwidth of the original single antenna ranges between 3.4-13.5 GHz; all the investigated MIMO antennas are laying around this bandwidth. Most of the investigated MIMOs start before and end after this bandwidth, and the relative bandwidth of all investigated antennas is around the relative bandwidth of the original single antenna which is 119.5. Some of their values exceed the previously mentioned value, reaching the maximum for the 2x1 inverted MIMO at about 169.6, whereas for the 2x2 nearby inverted MIMOs it reaches 141.2. As seen form Table 2, 2x1 inverted MIMO gives the best UWB bandwidth with the best relative gain, which gives a perspective to use this type of antenna for higher operating frequencies. In this work, we are not investigating enhancement of the bandwidth, but this antenna could be studied separately for this type of research.

Table 2. Comparison between a single antenna and all investigated antennas

Antenna	Operating bandwidth GHz	Resonant frequencies GHz	Relative BW (%)
Single antenna	3.4-13.5	3.9, 6.77, 10.3	119.5
2×1 inverted MIMO	3.28-40	4.28, 6.7, 9.1, 12.6, 16.14, 24.4, 27.7, 32.6, 36.8, 40	169.6
2×1 mirrored MIMO	3.5-12.67	3.9, 6, 6.6, 9.32, 10.6	113.4
2×1 nearby MIMO	3.18-14	3.67, 5.4, 6.82, 8.95, 10.1, 12.84	126
2×2 loop MIMO	3.48-12.5	4.07, 5.65, 6.5, 8.19, 9.6, 11.4	112.9
2×2 mirrored MIMO	3.12-13.68	3.8, 5.4, 6.7, 8.8, 9.85, 12.9	125.7
2×2 T-Mirrored MIMO	S_{11}	3.4-13.5	3.8, 6.8, 8.45, 10, 11, 13
	S_{22}	2.85-13.74	3.18, 5, 6.8, 9, 12.9
	S_{33}, S_{44}	3.15-13.95	3.6, 5.75, 6.8, 9, 10, 12.96
2×2 T- mirrored center inverted MIMO	S_{11}	3.34-13.54	4.1, 6.16, 6.9, 10, 11.36, 13
	S_{22}	3.4-15	3.25, 5.35, 6.7, 9, 12.8, 15
	S_{33}, S_{44}	3.15-15	3.8, 4.7, 5.6, 6.7, 9.15, 12.5, 15
2×2 nearby MIMO	S_{11}, S_{22}	2.88-13.95	3.2, 5, 7, 9, 9.76, 13.9
	S_{33}, S_{44}	3.16-14.2	3.64, 5.15, 6.7, 9, 10, 12.83
	S_{11}, S_{22}	3-15	3.34, 5.37, 6.7, 9, 12.8, 15
2×2 nearby inverted MIMO	S_{11}, S_{22}	3.15-15	3.8, 5.6, 6.8, 9.12, 15
	S_{33}, S_{44}	3.44-14.2	4.07, 6.04, 7, 10.2, 11.4,
	S_{11}, S_{22}	3.35-12.66	4.06, 6.23, 9.7, 11.9
2×2 plus-shaped MIMO	S_{11}, S_{22}	3.13-13.6	3.9, 5.64, 6.7, 9, 10.45, 12.14
	S_{33}, S_{44}	3.36-13.5	3.9, 6.7, 10.25, 12.9
	S_{11}, S_{22}		

4.2. Relative gain

Figure 43 shows the comparison between the original single antenna and 2×1 MIMO antennas, where the worst case was received for mirrored MIMO. While the inverted MIMO gives the best results, portions of bandwidth 8.82 to 10.1 GHz and 13.45 to 15 GHz received gain is less than the single antenna. In Table 3, gain comparison for selected frequencies is listed.

From Table 3, it is evident that the maximum gain improvement is about 1.37 dB. Next, there is a comparison between the single antenna and all 2×2 MIMO antennas as shown in Figure 44, to evaluate the worst and the best-released gain received. A T-shaped MIMO antenna received the worst one as its gain was equal or less than the single antenna except for portions of bandwidth 7.24 to 8.65 GHz, and 13.9 to 15 GHz, where the maximum improvement in these portions was about 0.75 dB. The gain received for MIMO antennas was better than a single antenna until 9.1, 9, 8.7, 9.67, 9.1, 9.22, and 8.9 GHz for plus-shaped, chair-shaped, mirrored, nearby, nearby inverted, loop, and T-shaped inverted respectively. For the best visualization of the received results of the improved gain comparison between all MIMO antennas and the single antenna, the received gain for a selected frequency is listed in Table 4.

From Table 4, it is evident that the worst released gain improvement was received for T-shaped and T-shaped inverted MIMO antennas followed by nearby inverted, mirrored, and nearby respectively. From Table 4, it is notable that the best-released gain received was for plus-shaped, loop, and chair-shaped respectively. The maximum gain improvement received was 3.07 dB at resonant frequency 8.2 GHz for chair-shaped, whereas at this frequency 1.65 dB was received for both plus-shaped and loop antennas.

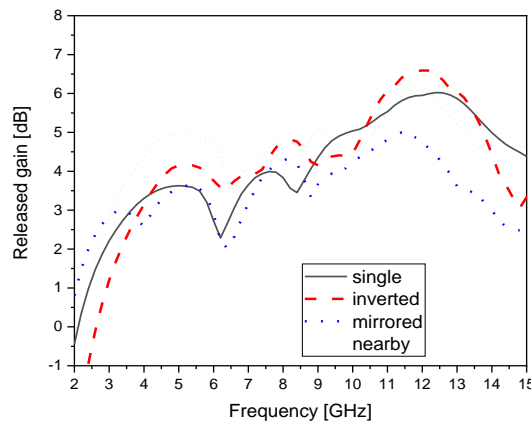


Figure 43. Comparison of the released gain between the single antenna and all 2×1 MIMO investigated antennas

Table 3. Gain comparison between single and 2x1 inverted MIMO antennas

Frequency [GHz]	Single antenna [dB]	2x1 inverted MIMO antenna [dB]	Gain improvement [dB]
3.4	2.63	4	+1.37
4.7	3.6	4.91	+1.31
6.2	2.32	3.47	+1.15
8	3.87	5.13	+1.26
8.82	4.10	4.10	0
9.2	4.61	3.71	-0.9
10.1	5.05	5.05	0
11.5	5.8	6.51	+0.71
13.45	5.5	5.5	0

The best gain for plus-shaped received was 2.73 dB at 4.2 GHz, whereas 1.17 and 0.92 dB were received for loop and chair-shaped respectively. Finally, the best-released gain for loop received 2.4 dB at 3 and 3.85 GHz resonant frequencies at these frequencies plus-shaped received 1.24, 2.4 dB respectively; however, chair-shaped received 0.38 and 0.25 dB respectively at these frequencies. The average improvement received was 1.81, 1.45, and 1.27 dB for plus-shaped, loop, and chair-shaped respectively.

From the received simulation we conclude that the plus-shaped, loop and the chair-shaped MIMO antennas give the best results of released gain. Depending on the purpose of using the antenna in terms of the required narrowband frequencies within the UWB range and the purpose of this use, any of the antennas can be used to increase the gain for narrow frequencies without the need to increase the radiated power.

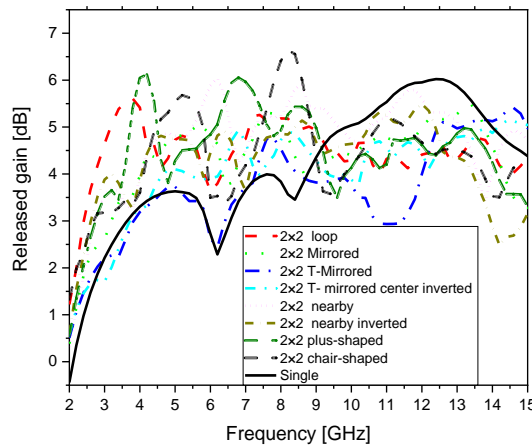


Figure 44. Comparison the released gain between the single antenna and all 2x2 MIMO investigated antennas

Table 4. The improved gain comparison between all MIMO antennas and the single antenna

Freq GHz	Single antenna	Plus-shaped		Chair-shaped		Mirrored		Nearby		Nearby inverted		Loop		T-shaped		T-shaped inverted	
		dB	Imp.	dB	Imp.	dB	Imp.	dB	Imp.	dB	Imp.	dB	Imp.	dB	Imp.	dB	Imp.
3	2.27	3.55	1.28	3.14	0.87	2.62	0.35	3.54	1.27	2.27	0	4.67	2.4	2.64	0.37	1.72	-0.55
3.85	3.15	5.55	2.4	3.4	0.25	3.62	0.47	3.44	0.29	3.15	0	5.55	2.4	3.04	-0.11	3.15	0
4.2	3.43	6.16	2.73	4.35	0.92	4.42	0.99	4.42	0.99	4.42	0.99	4.6	1.17	3.3	-0.13	3.32	-0.11
4.5	3.54	5	1.46	5	1.46	4.47	0.93	4.83	1.29	4.75	1.21	4.35	0.81	3.54	0	3.83	0.29
5.2	3.6	4.51	0.91	5.7	2.1	4.85	1.25	4.7	1.1	4.7	1.1	4.82	1.22	3.6	0	4.04	0.44
6.2	2.35	5	2.65	3.53	1.18	4.63	2.28	6.04	3.69	4.83	2.48	3.85	1.5	2.35	0	3.95	1.6
6.8	3.4	6	2.6	4	1.6	4.23	0.83	4.23	0.83	4	1.6	4.66	1.26	3.57	0.17	4.94	1.54
8.2	3.55	5.20	1.65	6.62	3.07	4.8	1.25	5.5	1.95	4.87	1.32	5.20	1.65	4.22	0.67	4.86	1.31
9	4.35	4.92	0.57	4.35	0	4.08	-0.27	5.36	10.1	4.7	0.25	4.96	0.61	3.82	-0.53	4.3	-0.05

In Table 5, comparisons are made with other works to compare the received results. From Table 5, it is evident that the proposed antennas are perspective, essentially 2x1 inverted MIMO as its bandwidth is the largest without any mismatches in the whole interval; moreover, it could have more operating bandwidth than shown (not simulated more than 40 GHz). The other three best 2x2 MIMO antennas give good peak gain concerning the reported works, which seems to be good to use for UWB high gain without the need to increase the radiated power.

Table 5. Comparison between the proposed MIMO antennas and recent works

Ref.	Ant. Dimension [mm]	MIMO Antenna	Operating frequency [GHz]	Peak gain [dB] for MIMO Antenna
[12]	20 × 24	2×1	42.0 to 49.0	> 8
[18]	70 × 70	2×2	2 to 4.5	1.84-3.49
[27]	20×45	2×2	2.97 to 19.82	3.3-8.12
[28]	15×10.3	2×2	27 to 28.95	6.14
[29]	66 × 66	2×2	2.2 to 2.7	6.17
[30]	60 × 60	2×2	2.65 to 15	>6
This work	Inverted	2×1	3.28 to 40	6.51
	Plus-shaped	2×2	3.44 to 14.2	6.16
	loop	2×2	2.48 to 12.5	5.6
	Chair-shaped	2×2	3.13 to 13.6	6.62

5. CONCLUSION

A different configuration of UWB 2×1 and 2×2 MIMO micro strip patch antennas was proposed and compared with the single UWB patch antenna to increase the released gain without the need to increase the input power radiation, using different substrate dimensions and patch antenna placing. The best simulation results of the three proposed 2×1 MIMO antenna received was for the 2×1 inverted with high UWB and a bandwidth up to 40 GHz without any mismatches, in addition to a maximum gain up to 6.51 dB, with an average gain of more than a single antenna of about 1.27 dB. For 2×2 MIMO antennas, the best received gain compared with a single antenna gain were at 4.2 GHz about +2.73, +1.17, and +0.92 dB for plus-shaped, loop, and chair-shaped respectively. The proposed MIMO antennas are suitable for narrowband within the UWB such as WLAN, WiMAX, ARN, ITU-8, and X-Band without the need to increase the radiated power of the transmitter antenna.




REFERENCES

- [1] F. C. Commission, "Revision of Part 15 of the commission's rules regarding ultra-wideband transmission systems," First Report and Order, FCC 02, V48, 2002.
- [2] M. S. Soliman, M. O. Dwairi, I. I. M. A. Sulayman, and S. H. A. Almalki, "A comparative study for designing and modeling patch antenna with different electromagnetic CAD approaches," *International Journal on Communications Antenna and Propagation (IRECAP)*, vol. 6, no. 2, pp. 90–95, Apr. 2016, doi: 10.15866/irecap.v6i2.8718.
- [3] M. O. Dwairi, M. S. Soliman, A. A. Alahmadi, S. H. A. Almalki, and I. I. M. Abu Sulayman, "Design and performance analysis of fractal regular slotted-patch antennas for ultra-wideband communication systems," *Wireless Personal Communications*, vol. 105, no. 3, pp. 819–833, Apr. 2019, doi: 10.1007/s11277-019-06123-5.
- [4] M. O. A.-D. Soliman, A. Y. Hendi, M. S. Soliman, and M. A. Nisirat, "Design of a compact ultra-wideband antenna for super-wideband technology," in *2019 13th European Conference on Antennas and Propagation (EuCAP)*, 2019, pp. 1–4.
- [5] S. Alotaibi and A. A. Alotaibi, "Design of a planar tri-band Notch UWB antenna for X-band, WLAN, and WiMAX," *Engineering, Technology & Applied Science Research*, vol. 10, no. 6, pp. 6557–6562, Dec. 2020, doi: 10.48084/etasr.3904.
- [6] M. O. Al-Dwairi, "A planar UWB semicircular-shaped monopole antenna with quadruple band notch for WiMAX, ARN, WLAN, and X-Band," *International Journal of Electrical and Computer Engineering (IJECE)*, vol. 10, no. 1, pp. 908–918, Feb. 2020, doi: 10.11591/ijece.v10i1.pp908-918.
- [7] M. O. Al-Dwairi, A. Y. Hindi, M. S. Soliman, and M. F. Aljafari, "A compact UWB monopole antenna with penta band notched characteristics," *TELKOMNIKA (Telecommunication Computing Electronics and Control)*, vol. 18, no. 2, pp. 622–630, Apr. 2020, doi: 10.12928/telkomnika.v18i2.14542.
- [8] N. M. Awad and M. K. Abdelazeez, "Multislot microstrip antenna for ultra-wide band applications," *Journal of King Saud University - Engineering Sciences*, vol. 30, no. 1, pp. 38–45, Jan. 2018, doi: 10.1016/j.jksues.2015.12.003.
- [9] M. Rahman, W. T. Khan, and M. Imran, "Penta-notched UWB antenna with sharp frequency edge selectivity using combination of SRR, CSRR, and DGS," *AEU - International Journal of Electronics and Communications*, vol. 93, pp. 116–122, Sep. 2018, doi: 10.1016/j.aeue.2018.06.010.
- [10] M. Rahman and J.-D. Park, "The smallest form factor UWB antenna with quintuple rejection bands for IoT applications utilizing RSRR and RCSRR," *Sensors*, vol. 18, no. 3, Mar. 2018, doi: 10.3390/s18030911.
- [11] R. B. G., C. Thampi, and S. K. Mohammed, "A CPW feed UWB antenna with quad band notches," *International Research Journal of Engineering and Technology*, vol. 5, no. 3, pp. 2048–2053, 2018.
- [12] J.-T. Weng and Q.-X. Chu, "Wideband microstrip MIMO antenna for millimeter-wave applications," in *2017 Sixth Asia-Pacific Conference on Antennas and Propagation (APCAP)*, Oct. 2017, pp. 1–3, doi: 10.1109/APCAP.2017.8420888.
- [13] M. Alibakhshikenari *et al.*, "A comprehensive survey on 'various decoupling mechanisms with focus on metamaterial and metasurface principles applicable to SAR and MIMO antenna systems,'" *IEEE Access*, vol. 8, pp. 192965–193004, 2020, doi: 10.1109/ACCESS.2020.3032826.
- [14] M. Alibakhshikenari, B. S. Virdee, and E. Limiti, "Study on isolation and radiation behaviours of a 34×34 array-antennas based on SIW and metasurface properties for applications in terahertz band over 125–300 GHz," *Optik*, vol. 206, Mar. 2020, doi: 10.1016/j.ijleo.2019.163222.
- [15] M. Alibakhshikenari *et al.*, "Isolation enhancement of densely packed array antennas with periodic MTM-photonic bandgap for SAR and MIMO systems," *IET Microwaves, Antennas & Propagation*, vol. 14, no. 3, pp. 183–188, Mar. 2019, doi: 10.1049/iet-map.2018.5747.
- [16] M. Alibakhshikenari, M. Khalily, B. S. Virdee, C. H. See, R. A. Abd-Alhameed, and E. Limiti, "Mutual-coupling isolation using embedded metamaterial EM bandgap decoupling slab for densely packed array antennas," *IEEE Access*, vol. 7, pp. 51827–51840, 2019, doi: 10.1109/ACCESS.2019.2909950.




- [17] M. Alibakhshikenari, M. Khalily, B. S. Virdee, C. H. See, R. A. Abd-Alhameed, and E. Limiti, "Mutual coupling suppression between two closely placed microstrip patches using EM-bandgap metamaterial fractal loading," *IEEE Access*, vol. 7, pp. 23606–23614, 2019, doi: 10.1109/ACCESS.2019.2899326.
- [18] B. Y. V. N. R. Swamy and P. Siddaiah, "Design of a compact 2×2 multi band MIMO antenna for wireless applications," *International Journal of Recent Technology and Engineering (IJRTE)*, vol. 7, no. 6S2, pp. 674–683, 2019.
- [19] H. Li, T. Wei, J. Ding, and C. Guo, "A dual-band polarized diversity microstrip MIMO antenna with high isolation for WLAN application," in *2016 11th International Symposium on Antennas, Propagation and EM Theory (ISAPE)*, Oct. 2016, pp. 88–91, doi: 10.1109/ISAPE.2016.7833885.
- [20] A. Khan, S. Geng, X. Zhao, Z. Shah, M. U. Jan, and M. A. Abdelbaky, "Design of MIMO antenna with an enhanced isolation technique," *Electronics*, vol. 9, no. 8, Jul. 2020, doi: 10.3390/electronics9081217.
- [21] R. A. Sadeghzadeh, M. Alibakhshi-Kenari, and M. Naser-Moghadasi, "UWB antenna based on SCRLH-TLs for portable wireless devices," *Microwave and Optical Technology Letters*, vol. 58, no. 1, pp. 69–71, Jan. 2016, doi: 10.1002/mop.29491.
- [22] M. Alibakhshi-Kenari, M. Naser-Moghadasi, R. Ali Sadeghzadeh, and B. Singh Virdee, "Metamaterial-based antennas for integration in UWB transceivers and portable microwave handsets," *International Journal of RF and Microwave Computer-Aided Engineering*, vol. 26, no. 1, pp. 88–96, Jan. 2016, doi: 10.1002/mmce.20942.
- [23] M. Alibakhshi-Kenari, M. Naser-Moghadasi, and R. A. Sadeghzadeh, "Composite right–left-handed-based antenna with wide applications in very-high frequency–ultra-high frequency bands for radio transceivers," *IET Microwaves, Antennas & Propagation*, vol. 9, no. 15, pp. 1713–1726, Dec. 2015, doi: 10.1049/iet-map.2015.0308.
- [24] M. Alibakhshi-Kenari, M. Naser-Moghadasi, and R. A. Sadeghzadeh, "Bandwidth and radiation specifications enhancement of monopole antennas loaded with split ring resonators," *IET Microwaves, Antennas & Propagation*, vol. 9, no. 14, pp. 1487–1496, Nov. 2015, doi: 10.1049/iet-map.2015.0172.
- [25] M. Alibakhshi-Kenari, M. Naser-Moghadasi, and R. Sadeghzadeh, "The resonating MTM-based miniaturized antennas for wide-band RF-microwave systems," *Microwave and Optical Technology Letters*, vol. 57, no. 10, pp. 2339–2344, Oct. 2015, doi: 10.1002/mop.29328.
- [26] Q. Wang, N. Mu, L. Wang, S. Safavi-Naeini, and J. Liu, "5G MIMO conformal microstrip antenna design," *Wireless Communications and Mobile Computing*, vol. 2017, pp. 1–11, 2017, doi: 10.1155/2017/7616825.
- [27] H. Alsaif, "Extreme wide band MIMO antenna system for fifth generation wireless systems," *Engineering, Technology & Applied Science Research*, vol. 10, no. 2, pp. 5492–5495, Apr. 2020, doi: 10.48084/etasr.3413.
- [28] R. K. Goyal and U. S. Modani, "Compact MIMO microstrip patch antenna design at 28 GHz for 5G smart phones," *International Journal of Engineering Research & Technology (IJERT)*, vol. 9, no. 4, 2021, doi: 10.10757/IJERTCONV9IS04001.
- [29] R. S. Bhadade and S. P. Mahajan, "High gain circularly polarized pentagonal microstrip for massive MIMO base station," *Advanced Electromagnetics*, vol. 8, no. 3, pp. 83–91, Sep. 2019, doi: 10.7716/aem.v8i3.764.
- [30] M. O. Dwairi, "Increasing gain evaluation of 2×1 and 2×2 MIMO microstrip antennas," *Engineering, Technology & Applied Science Research*, vol. 11, no. 5, pp. 7531–7535, Oct. 2021, doi: 10.48084/etasr.4305.

BIOGRAPHIES OF AUTHORS






Majed Omar Dwairi    is a PhD communication system, was born on the 10 of December 1968 in Jordan. He received his diploma degree in 1994 and PhD degree from Ukraine state Academy in 1998 in the field of multichannel communication. An associate professor in the Department of Electrical Engineering, Faculty of Engineering Technology, Al-Balqa Applied University Amman, Jordan. His research interests include optical communication networks, digital communications, signal, and image processing, antenna design, and microstrip patch antennas. He can be contacted at email: majeddw@bau.edu.jo.






Mohamed Salaheldeen Soliman    An assistant professor in the Department of Electrical Engineering, Faculty of Energy Engineering, Aswan University, Egypt. Currently, he is with the Department of Electrical Engineering, Faculty of Engineering Taif University, Saudi Arabia. Dr. Soliman had his Ph.D. in Communications Engineering from the Graduate School of Engineering, Osaka University, Japan. He is the author and co-author of many research journals and conference articles. He was granted many research projects from the Deanship of Scientific Researches, Taif University, Saudi Arabia. His research interests include wireless communications, phased and timed array signal processing, UWB microstrip patch antennas, dielectric resonant antennas, numerical methods in electromagnetics, MIMO antenna, optimization techniques in antenna design, and antenna measurement techniques. He serves as a reviewer in many scientific journals (i.e PIER journals, International Journal of RF and Microwave Computer-Aided Engineering) and TPC member in many international conferences. Dr. Soliman is a senior member of IEEE-MTT/AP Society, KAUST chapter, Saudi Arabia. He can be contacted at email: soliman.comm.tu.ksa@gmail.com.



Amjad Yousef Hendi    is a PhD in Radio and Tv system. He received his diploma degree in 1994 and PhD degree from Ukraine state Academy in 1998 in the field of Radio & Tv systems. An associate professor in the department of Electrical Engineering, faculty of Engineering Technology, Al-Balqa Applied University Amman, Jordan. His research interests include digital communications, signal and image processing, Antenna design, optimization techniques in antenna design and antenna measurement techniques and microstrip patch antennas. He can be contacted at email: amjad_svyaz@yahoo.com.



Ziad AL-Qadi    is a PhD in computer engineering, was born on 09 March 1955 in Jordan. He received his diploma degree in 1980 and PhD degree from Ukraine in 1986 in the field of Computer Engineering. Currently he is a Professor at the Computer Engineering Department, Faculty of Engineering Technology, Al-Balqa Applied University, Jordan. His main interest includes signal processing, pattern recognition, algorithms, modelling, and simulations. He can be contacted at email: natalia_maw@yahoo.com.